Archive of Applied Mechanics (2023) 93:3313–3325
https://doi.org/10.1007/s00419-023-02440-1

ORIGINAL

Iqbal Kaur · Kulvinder Singh

Stoneley wave propagation in transversely isotropic thermoelastic rotating medium with memory-dependent derivative and two temperature

Received: 21 September 2022 / Accepted: 9 May 2023 / Published online: 3 June 2023

Abstract In the present paper, we bring forth the study of the propagation of the Stoneley wave with modified GN theory of type II thermoelasticity without energy dissipation, including memory-dependent derivative (MDD) and two temperatures and with rotation. Secular equations of Stoneley waves at the interface of two separate homogeneous transversely isotropic (HTI) thermoelastic mediums are determined in the form of determinants after constructing the formal solution based on the necessary boundary conditions. The wave characteristics have been obtained for different Kernel functions of the MDD from the secular equations and are depicted graphically. The effect of Kernel functions and two temperature has been depicted on the displacement component, Temperature distribution, stress component, phase velocity, and attenuation coefficient.

Keywords Transversely isotropic · Thermoelastic · Memory-dependent derivative · Stoneley wave propagation · Kernel function

List of symbols

e_{ij}	Strain tensors
$\overrightarrow{u}$	Displacement vector
K_{ij}^{*}	Materialistic constant
α_{ij}	Linear thermal expansion coefficient
$\delta(t)$	Dirac's delta function
$2\Omega \times \dot{u}$	Coriolis acceleration
τ_0	Relaxation time
t_{ij}	Stress tensors
δ_{ij}	Kronecker delta
u_i	Components of displacement
a_{ij}	Two temperature parameters
C_E	Specific heat
ξ	Wavenumber
β_{ij}	Thermal elastic coupling tensor
ω	Angular frequency
$\boldsymbol{\Omega}$	Angular velocity of the solid and equal to $\Omega \boldsymbol{n}$, where $\mathbf{n}$ is a unit vector

I. Kaur (✉)
Department of Mathematics, Government College for Girls, Palwal, Kurukshetra, India
e-mail: bawahanda@gmail.com

K. Singh
Faculty of Engineering, UIET, Kurukshetra University, Haryana, India
e-mail: ksingh2015@kuk.ac.in

C_{ijkl}	Elastic parameters
F_i	Components of Lorentz force
φ	Conductive temperature
ε_0	Electric permeability
T_0	Reference temperature
T	Absolute temperature
C_1	Longitudinal wave velocity
ρ	Medium density

1 Introduction

A Stoneley wave is an interface wave that often moves along the boundary between two solids. Due to the existence of homogeneities in the crust of the earth and the fact that the earth is made up of several layers, the propagation of surface waves in a homogeneous elastic media is of significant importance in the fields of earthquake engineering and seismology. Furthermore, this wave is called a Scholte wave if it originates at the interface between such a liquid and a solid. The intensity of the Stoneley wave is maximum at the boundary and exponentially diminishes away from it. One example of these waves is the wave produced by a sonic tool in a bore well. The Stoneley wave study reveals details regarding the locations of fractures and formation permeability. These waves assist appraise valuable resources beneath the surface of the earth and provide better knowledge of the interior structure of the planet. In vertical seismic profiles, Stoneley waves are a prominent source of background noise.

In 1924, it was Stoneley who developed the theory of surface waves. Stoneley [1] developed the Stoneley wave's dispersion equation after initially examining the occurrence of these waves propagating at the interface of two solid, solid–liquid media. Scholte [2] investigated a wave similar to the Stoneley wave known as the Scholte wave that originates at the fluid–solid interfaces. Stoneley waves were investigated by Tajuddin [3] at the intersection of two micropolar elastic half-spaces. In the context of different theories of thermoelasticity, Kumar et al. [4] examined the Stoneley waves at the interface of isotropic modified coupling stress thermoelastic with mass diffusion media.

In the following years, several researchers have discussed problems regarding Stoneley waves propagating along solid–solid and fluid–solid boundaries, such as Ting [5], Abo-Dahab [6, 7], Kumar et al. [8], Abd-Alla et al. [9], Singh and Tochhawng [10], Kaur and Lata [11], Lata and Himanshi [12], Kaur et al. [13, 14], Kaur and Singh [15] and Lata et al. [16].

In addition, A common derivative and kernel function is used to define the MDD in integral form. In many models that explain physical terms with the memory effect, the kernels in physical laws are crucial. The idea of an MDD was first presented by Wang and Li [17] in 2011. When calculating the heat flux rate in the Lord–Shulman (LS) generalized thermoelasticity theory, Yu et al. [18] developed the MDD as an alternative to fractional calculus to reflect memory dependence and be recognized as a memory-dependent LS model. The following reasons suggest that this novel model may be advantageous to fractional models. First, the shape of the new model is distinct from that of the fractional-order models, which have different modifications. The substance of the MDD definition also makes the physical significance of the new model more obvious. Third, the new model is more practical for numerical calculation than fractional models since it is represented by differentials and integrals of integer order. As a result, the model is more adaptable in applications than fractional models, in which the significant variable is the fractional-order parameter. The kernel function and time delay of the MDD can also be changed arbitrarily. Ezzat et al. [19–22] discussed the MDD LS model of generalized thermoelasticity was used to solve a few one-dimensional problems. Although this is true, different researchers have developed varying theories of thermoelasticity, such as Kaur et al. [23–26], Marin [27], and [28], Marin et al. [29, 30], Kaur et al. [31], Golewski [32, 33], Trivedi et al. [34], Zhang et al. [35], Sur and Kanoria [36], Golewski [37, 38], Gupta et al. [39]. Chandrasekharaiah [40], and Green and Naghdi [41].

In this paper, Stoneley wave propagation with the memory-dependent derivative (MDD) has been studied. Secular equations of Stoneley waves at the interface of two separate homogeneous transversely isotropic (HTI) thermoelastic media are determined in the form of determinants after constructing the formal solution based on the necessary boundary conditions. The wave characteristics have been obtained for different Kernel functions of the MDD and are depicted graphically.

2 Basic equations

The fundamental governing equations for homogeneous, anisotropic, generalized thermoelastic and without body forces are.

- *Equation of motion with rotation*

Following Schoenberg and Censor [42] for rotating solids with a uniform angular velocity Ω we have,

$$t_{ij,j} = \rho\left\{\ddot{\boldsymbol{u}}_i + (\boldsymbol{\Omega} \times (\boldsymbol{\Omega} \times \mathbf{u}))_i + (2\boldsymbol{\Omega} \times \dot{\boldsymbol{u}})_i\right\}, \tag{1}$$

The terms $\boldsymbol{\Omega} \times (\boldsymbol{\Omega} \times \mathbf{u})$ represent the centripetal acceleration due to the time-varying motion.

- *Constitutive equations*

Following Youssef [43], the constitutive equations for anisotropic solids with two temperature theory are

$$t_{ij} = C_{ijkl}e_{kl} - \beta_{ij}T, \tag{2}$$

$$e_{ij} = \frac{1}{2}\left(u_{i,j} + u_{j,i}\right), \quad i, j = 1, 2, 3, \tag{3}$$

$$T = \varphi - a_{ij}\varphi_{,ij}, \tag{4}$$

$$\beta_{ij} = C_{ijkl}\alpha_{kl}, \tag{5}$$

Here $C_{ijkl} = C_{klij} = C_{jikl} = C_{ijlk}$.

- *Heat conduction equation*

Following Youssef [43], Bachher [44] the heat conduction equation without energy dissipation, two temperature theory and with memory-dependent derivatives is

$$K_{ij}^{*}\varphi_{,ij} = \left(1 + \chi D_{\chi}\right)\left(\beta_{ij}T_0\ddot{e}_{ij} + \rho C_E\ddot{T}\right), \tag{6}$$

Following Wang and Li [17], for a first-order MDD for a differentiable function $f(t)$ with delay $\chi > 0$ for a fixed time t is:

$$D_{\chi} f(t) = \frac{1}{\chi}\int_{t-\chi}^{t} K(t - \xi) f'(\xi)\, \mathrm{d}\xi, \tag{7}$$

The choice of the kernel function, $K(t - \xi)$ and time delay parameter, χ are determined by the material properties. Following Ezzat et al. [19–21] the kernel function $K(t - \xi)$ is taken here in the form

$$K(t-\xi) = 1 - \frac{2\beta}{\chi}(t-\xi) + \frac{\alpha^2}{\chi^2}(t-\xi)^2 = \begin{cases} 1 & \alpha = 0, \beta = 0, \\ 1 + (\xi - t)/\chi & \alpha = 0, \beta = 1/2, \\ \xi - t + 1 & \alpha = 0, \beta = \chi/2, \\ [1 + (\xi - t)/\chi]^2 & \alpha = 1, \beta = 1. \end{cases} \tag{8}$$

where α and β are constants. Additionally, the comma indicates the derivative *w.r.t.* the space variable and the dot superimposed on it signifies the time derivative.

3 Formulation of the problem

We take into account two homogeneous, transversely isotropic thermoelastic rotating half-spaces M_1 and M_2, both of which are perfectly conducting. These half-spaces are connected at the interface $z = 0$. The coordinate system's (x, y, z) origin is taken to be at $(z = 0)$. Displacement vector $\overrightarrow{u}$ has the components u, v, w along x, y, z-axis, respectively. We select the x-axis in the wave propagation direction such that all particles on a line parallel to the y-axis are equally displaced, ensuring that $v = 0$andu, w, are independent of y. The regions $-\infty < x \leq 0$ and $0 \leq x < \infty$ are occupied by the media M_1 and M_2, respectively. The plane represents the separation between the two mediums, M_1 and M_2. The quantities symbolized are without a bar for the media M_1 and with a bar for media M_2. For the 2D problem in xz-plane, we consider (Fig. 1)

$$\boldsymbol{u} = (u, 0, w). \tag{9}$$

Following Slaughter [45], Eqs. (1) and (6) can now be transformed as follows:

$$C_{11}\frac{\partial^2 u}{\partial x^2} + C_{13}\frac{\partial^2 w}{\partial x \partial z} + C_{44}\left(\frac{\partial^2 u}{\partial z^2} + \frac{\partial^2 w}{\partial x \partial z}\right) - \beta_1 \frac{\partial}{\partial x}\left\{\varphi - \left(a_1\frac{\partial^2 \varphi}{\partial x^2} + a_3\frac{\partial^2 \varphi}{\partial z^2}\right)\right\} = \rho\left(\frac{\partial^2 u}{\partial t^2} - \Omega^2 u + 2\Omega\frac{\partial w}{\partial t}\right), \tag{10}$$

$$(C_{13} + C_{44})\frac{\partial^2 u}{\partial x \partial z} + C_{44}\frac{\partial^2 w}{\partial x^2} + C_{33}\frac{\partial^2 w}{\partial z^2} - \beta_3 \frac{\partial}{\partial z}\left\{\varphi - \left(a_1\frac{\partial^2 \varphi}{\partial x^2} + a_3\frac{\partial^2 \varphi}{\partial z^2}\right)\right\} = \rho\left(\frac{\partial^2 w}{\partial t^2} - \Omega^2 w - 2\Omega\frac{\partial u}{\partial t}\right), \tag{11}$$

$$K_1^*\frac{\partial^2 \varphi}{\partial x^2} + K_3^*\frac{\partial^2 \varphi}{\partial z^2} = \left(1 + \chi D_\chi\right)\left[\rho C_E\frac{\partial^2}{\partial t^2}\left\{\varphi - \left(a_1\frac{\partial^2 \varphi}{\partial x^2} + a_3\frac{\partial^2 \varphi}{\partial z^2}\right)\right\} + T_0\left\{\beta_1\frac{\partial \ddot{u}}{\partial x} + \beta_3\frac{\partial \ddot{w}}{\partial z}\right\}\right] \tag{12}$$

and

$$t_{xx} = C_{11}e_{xx} + C_{13}e_{xz} - \beta_1\left\{\varphi - \left(a_1\frac{\partial^2 \varphi}{\partial x^2} + a_3\frac{\partial^2 \varphi}{\partial z^2}\right)\right\}, \tag{13}$$

$$t_{zz} = C_{13}e_{xx} + C_{33}e_{zz} - \beta_3\left\{\varphi - \left(a_1\frac{\partial^2 \varphi}{\partial x^2} + a_3\frac{\partial^2 \varphi}{\partial z^2}\right)\right\}, \tag{14}$$

$$t_{xz} = 2C_{44}e_{xz}, \tag{15}$$

where

$$\beta_1 = (C_{11} + C_{12})\alpha_1 + C_{13}\alpha_{3,} \tag{16}$$

$$\beta_3 = 2C_{13}\alpha_1 + C_{33}\alpha_3, \tag{17}$$

$a_1 \& a_3$ are two temperature parameters. In the above equations, we use the contracting subscript notations $(1 \rightarrow 11, 2 \rightarrow 22, 3 \rightarrow 33, 5 \rightarrow 23, 4 \rightarrow 13, 6 \rightarrow 12)$ to relate C_{ijkl} to C_{mn}.

Using dimensionless quantities:

$$\left(x', z'\right) = \frac{1}{L}(x, z,), \left(u', w'\right) = \frac{\rho C_1^2}{L\beta_1 T_0}(u, w), \rho C_1^2 = C_{11}, \left(T', \varphi'\right) = \frac{1}{T_0}(T, \varphi),$$
$$t' = \frac{C_1}{L}t,\ \left(t'_{xx},\ t'_{zx}t'_{zz}\right) = \frac{1}{\beta_1 T_0}(t_{xx},\ t_{zx},\ t_{zz}),\ \left(a'_1,\ a'_3\right) = \frac{1}{L^2}(a_1,\ a_3),\ \Omega' = \frac{\mathrm{L}}{C_1}\Omega. \tag{18}$$

Suppressing the primes and utilizing (18) in Eqs. (10)–(12), we obtain

$$\frac{\partial^2 u}{\partial x^2} + \delta_2\frac{\partial^2 w}{\partial x \partial z} + \delta_1\frac{\partial^2 u}{\partial z^2} - \frac{\partial}{\partial x}\left\{\varphi - \left(a_1\frac{\partial^2 \varphi}{\partial x^2} + a_3\frac{\partial^2 \varphi}{\partial z^2}\right)\right\} = \left(\frac{\partial^2 u}{\partial t^2} - \Omega^2 u + 2\Omega\frac{\partial w}{\partial t}\right), \tag{19}$$

$$\delta_2\frac{\partial^2 u}{\partial x \partial z} + \delta_1\frac{\partial^2 w}{\partial x^2} + \delta_3\frac{\partial^2 w}{\partial z^2} - \delta_5\frac{\partial}{\partial z}\left\{\varphi - \left(a_1\frac{\partial^2 \varphi}{\partial x^2} + a_3\frac{\partial^2 \varphi}{\partial z^2}\right)\right\} = \left(\frac{\partial^2 w}{\partial t^2} - \Omega^2 w - 2\Omega\frac{\partial u}{\partial t}\right), \tag{20}$$

$$\left(\frac{\partial^2 \varphi}{\partial x^2} + \delta_6\frac{\partial^2 \varphi}{\partial z^2}\right) = \left(1 + \chi D_\chi\right)\left[\delta_8\frac{\partial^2}{\partial t^2}\left\{\varphi - \left(a_1\frac{\partial^2 \varphi}{\partial x^2} + a_3\frac{\partial^2 \varphi}{\partial z^2}\right)\right\} + \delta_7\left\{\frac{\partial u}{\partial x} + \delta_5\frac{\partial w}{\partial z}\right\}\right], \tag{21}$$

where

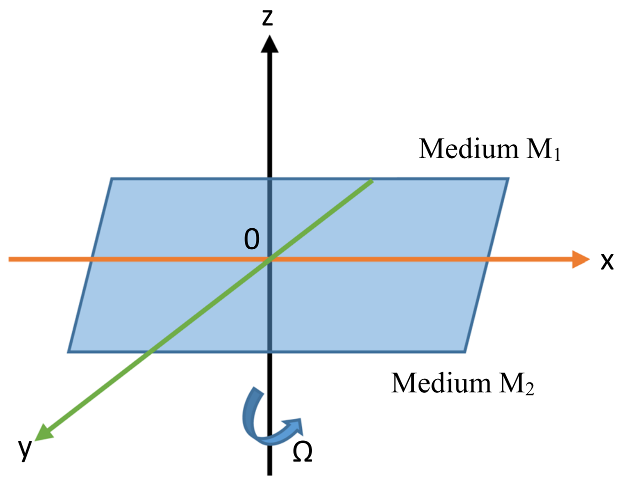

Fig. 1 Geometry of the problem

$$\delta_1 = \frac{c_{44}}{c_{11}},\ \delta_2 = \frac{c_{13}+c_{44}}{c_{11}},\ \delta_3 = \frac{c_{33}}{c_{11}},\ \delta_5 = \frac{\beta_3}{\beta_1},\ \delta_6 = \frac{K_3^*}{K_1^*},\ \delta_7 = \frac{T_0\beta_1^2}{K_1^*\rho},\ \delta_8 = \frac{C_E C_{11}}{K_1^*}.$$

We consider the solution of the form

$$(u, w, \varphi) = \left(u^*, w^*, \varphi^*\right)(z)e^{i\xi(x-ct)}, \tag{22}$$

where $c = \omega/\xi$ represents the dimensionless phase velocity.

After applying (22) in Eqs. (19)–(21) yields

$$u^*\left[l_1 + \delta_2 D^2\right] + w^*[l_2 + l_3 D] + \varphi^*\left[l_4 + l_5 D^2\right] = 0, \tag{23}$$

$$u^*[-l_2 + l_3 D] + w^*\left[l_6 + \delta_3 D^2\right] + \varphi^*\left[l_7 D + l_8 D^3\right] = 0, \tag{24}$$

$$u^*[l_9] + w^*[l_{10} D] + \varphi^*\left[l_{11} + l_{12} D^2\right] = 0, \tag{25}$$

where

$$l_1 = \xi^2\left(c^2 - 1\right),\ l_2 = 2i\xi c,\ l_3 = \delta_2 i\xi,\ l_4 = -i\xi\left(1 + a_1\xi^2\right),\ l_5 = a_3 i\xi,$$

$$l_6 = \left(c^2 - \delta_1\right)\xi^2 + 1,\ l_7 = -\delta_5\left(1 + a_1\xi^2\right),\ l_8 = \delta_5 a_3,\ l_9 = (1+G)\delta_7 i\xi^3 c^2,\ l_{10} = (1+G)\delta_7\delta_5\xi^2 c^2,$$

$$l_{11} = \delta_8\xi^2 c^2\left(1 + a_1\xi^2\right) - \xi^2,\ l_{12} = -\delta_8\xi^2 c^2 a_3 + \delta_6.$$

$$G = \frac{1}{\chi}\left[\left(1 - e^{i\xi c\chi}\right)\left(1 + \frac{2\beta}{\chi i\xi c} - \frac{2\alpha^2}{\chi^2\xi^2 c^2}\right) - \left(\alpha^2 - 2\beta - \frac{2\alpha^2}{\chi i\xi c}\right)e^{i\xi c\chi}\right]$$

and characteristic equation in the form of a biquadratic equation represented in D^2 given by

$$D^6 + \frac{B}{A}D^4 + \frac{C}{A}D^2 + \frac{E}{A} = 0, \tag{26}$$

where

$$\begin{aligned} A &= \delta_2\delta_3 l_{12} - l_{10}\delta_2 l_8, \\ B &= \delta_3\delta_2 l_{11} + \delta_2 l_6 l_{12} + l_1\delta_3 l_{12} - \delta_2 l_{10} l_7 - l_1 l_{10} l_8 \\ &\quad - l_1^2 l_{12} + l_8 l_9 l_3 + l_3 l_5 l_{10} - l_5\delta_3 l_9, \\ C &= \delta_2 l_{11} l_6 + l_{11}\delta_3 l_1 + l_1 l_6 l_{12} - l_1 l_{10} l_7 + l_1^2 l_{11} + l_2^2 l_{12} - l_3^2 l_{11} \end{aligned}$$

$$+l_3l_9l_7+l_3l_4l_{10}-l_5l_9l_6-l_4\delta_3l_9,$$
$$E=l_{11}l_1l_6-l_9l_4l_6.$$

For medium M_1

$$(u,w,\varphi)=\sum_{j=1}^{3}A_j\left(1,d_j,k_j\right)e^{-m_jz}e^{i\xi(x-ct)},\tag{27}$$

Thus from Eqs. (22) and (27)

$$u^*=\sum_{j=1}^{3}A_je^{-m_jz},$$
$$w^*=\sum_{j=1}^{3}d_jA_je^{-m_jz},$$
$$\varphi^*=\sum_{j=1}^{3}k_jA_je^{-m_jz},$$

where

$$d_j=\frac{l_1l_{11}-l_9\mathrm{l}_4+(l_{11}\delta_2+l_1\mathrm{l}_{12}-l_9\mathrm{l}_5)m_j^2+(\delta_2l_{12})m_j^4}{l_6l_{11}+(l_{11}\delta_3+l_6\mathrm{l}_{12}-l_{10}\mathrm{l}_7)m_j^2+(\delta_3l_{12}-l_{10}\mathrm{l}_8)m_j^4},\tag{28}$$
$$k_j=\frac{l_1l_6+l_2^2+\left(l_6\delta_2+l_1\delta_3-l_3^2\right)m_j^2+(\delta_2\delta_3)m_j^4}{l_6l_{11}+(l_{11}\delta_3+l_6\mathrm{l}_{12}-l_{10}\mathrm{l}_7)m_j^2+(\delta_3l_{12}-l_{10}\mathrm{l}_8)m_j^4}.\tag{29}$$

For medium M_2 ($z>0$) we will attach a bar

$$(\overline{u},\overline{w},\overline{\varphi})=\left(1,\overline{d_j},\overline{k_j}\right)e^{\overline{m_j}z}\overline{A_j}e^{i\xi(x-ct)},\tag{30}$$

where quantities $\overline{u}$, $\overline{w}$, $\overline{\varphi}$,$\overline{d_j}$, $\overline{k_j}$,$\overline{A_j}$,$\overline{m_j}$ are obtained by attaching bars in the above expressions.

4 Boundary conditions

We assume that there is perfect contact between the two half-spaces. As a result, the Stoneley wave characteristics are stable at the interface.

Following are the boundary conditions at $z=0$:

$$t_{zz}=\bar{t}_{zz},t_{zx}=\bar{t}_{zx},\varphi=\overline{\varphi},u=\overline{u},w=\overline{w},K_3^*\frac{\partial\varphi}{\partial z}=\overline{K_3^*}\frac{\partial\overline{\varphi}}{\partial z}.\tag{31}$$

5 Derivations of the secular equations

With the values of u, w, φ, $\overline{u}$, $\overline{w}$, $\overline{\varphi}$ in (31), it yields six linear equations:

$$\sum_{j=1}^{3}Q_{pj}A_j+\sum_{j=1}^{3}Q_{p(j+3)}\overline{A}_j=0,\quad p=1,2,3,4,5,6.\tag{32}$$

where

$$Q_{1j}=i\xi-\delta_9d_jm_j-\left(1+a_1\xi^2-a_3m_j^2\right)k_j,$$
$$Q_{1(j+3)}=-i\xi-\delta_9\overline{d_j}\overline{m_j}+\left(1+a_1\xi^2-a_3\overline{m_j^2}\right)\overline{k_j},$$

$$
\begin{aligned}
Q_{2j} &= -m_j + d_j i\xi, Q_{2(j+3)} = -m_j - d_j i\xi, \\
Q_{3j} &= k_j, Q_{3(j+3)} = -\overline{k_j}, \\
Q_{4j} &= \delta_1 m_j^2 + \left(2i\xi c - \delta_2 i\xi m_j\right)d_j + \left(-i\xi\left(1 + a_1\xi^2\right) + a_3 i\xi m_j^2\right)k_j, \\
Q_{4(j+3)} &= -\delta_1\overline{m_j^2} - \left(2i\xi c - \delta_2 i\xi \overline{m}_j\right)d_j - \left(-i\xi\left(1 + a_1\xi^2\right) + a_3 i\xi\overline{m_j^2}\right)\overline{k_j}, \\
Q_{5j} &= -2\delta_4 i\xi c - \delta_2 i\xi m_j + \delta_3 m_j^2 d_j - \delta_5\left(-\left(1 + a_1\xi^2\right)m_j + a_3 m_j^3\right)k_j, \\
Q_{5(j+3)} &= 2\delta_4 i\xi c - \delta_2 i\xi\overline{m_j} + \delta_3\overline{m_j^2}\overline{d_j} + \delta_5\left(-\left(1 + a_1\xi^2\right)\overline{m_j} + a_3\overline{m_j^3}\right)\overline{k_j}, \\
Q_{6j} &= -K_3^*\overline{k_j}\overline{m_j}.
\end{aligned} \tag{33}
$$

The system of Eq. (33) has a non-trivial solution if the determinant of unknowns A_j, $\overline{A}_j$, $j = 1, 2, 3$ vanishes, i.e.,

$$\left|Q_{ij}\right|_{6\times 6} = 0. \tag{34}$$

The attenuation coefficient, wavenumber, and phase velocity of Stoneley waves in the TIT medium are completely described by these secular Eq. (34).

6 Particular cases

If $C_{11} = C_{33} = \lambda + 2\mu$, $C_{12} = C_{13} = \lambda$, $C_{44} = \mu$, $\alpha_1 = \alpha_3 = \alpha'$, $\beta_1 = \beta_3 = \beta$, $K_1^* = K_3^* = K^*$ we get Stoneley wave propagation equations for isotropic materials with MDD with two temperature and rotation.

7 Numerical results and discussion

This section presents numerical results that illustrate the theoretical results and the effects of MDD. Copper material was chosen as medium 1 according to Kumar et al. [46].

Quantity	Value	Unit
c_{11}	18.78×10^{10}	$\mathrm{Kgm^{-1}s^{-2}}$
c_{12}	8.76×10^{10}	$\mathrm{Kgm^{-1}s^{-2}}$
c_{33}	17.2×10^{10}	$\mathrm{Kgm^{-1}s^{-2}}$
c_{13}	8.0×10^{10}	$\mathrm{Kgm^{-1}s^{-2}}$
c_{44}	5.06×10^{10}	$\mathrm{Kgm^{-1}s^{-2}}$
β_1	7.543×10^{6}	$\mathrm{Nm^{-2}deg^{-1}}$
β_3	9.208×10^{6}	$\mathrm{Nm^{-2}deg^{-1}}$
ρ	8.954×10^{3}	$\mathrm{Kgm^{-3}}$
C_E	4.27×10^{2}	$\mathrm{jKg^{-1}deg^{-1}}$
$K_1{}^*$	0.04×10^{2}	$\mathrm{Ns^{-2}deg^{-1}}$
$K_3{}^*$	0.02×10^{2}	$\mathrm{Ns^{-2}deg^{-1}}$
T_0	293	deg
α_1	2.98×10^{-5}	$\mathrm{K^{-1}}$
α_3	2.4×10^{-5}	$\mathrm{K^{-1}}$

Magnesium material [46], has been taken for medium 2, thermoelastic material as

Quantity	Value	Unit
$\overline{c}_{11}$	5.974×10^{10}	$\text{Kgm}^{-1}\text{s}^{-2}$
$\overline{c}_{12}$	2.624×10^{10}	$\text{Kgm}^{-1}\text{s}^{-2}$
$\overline{c}_{33}$	6.17×10^{10}	$\text{Kgm}^{-1}\text{s}^{-2}$
$\overline{c}_{13}$	2.17×10^{10}	$\text{Kgm}^{-1}\text{s}^{-2}$
$\overline{c}_{44}$	3.278×10^{10}	$\text{Kgm}^{-1}\text{s}^{-2}$
$\overline{\beta}_1$	2.68×10^{6}	$\text{Nm}^{-2}\text{deg}^{-1}$
$\overline{\beta}_3$	2.68×10^{6}	$\text{Nm}^{-2}\text{deg}^{-1}$
$\overline{\rho}$	1.74×10^{3}	Kgm^{-3}
$\overline{C}_E$	1.04×10^{3}	$\text{jKg}^{-1}\text{deg}^{-1}$
$\overline{K}_1^*$	0.02×10^{2}	$\text{Ns}^{-2}\text{deg}^{-1}$
$\overline{K}_3^*$	0.02×10^{2}	$\text{Ns}^{-2}\text{deg}^{-1}$
$\overline{T}_0$	293	deg
$\overline{\alpha}_1$	2.98×10^{-5}	K^{-1}
$\overline{\alpha}_3$	2.4×10^{-5}	K^{-1}

The graphical representations of stress components, temperature change, wave velocity, and attenuation coefficient have been explored with MDD and two temperature (2T) using the aforementioned data and are illustrated graphically as:

7.1 Effect of MDD and 2T

1. The solid line corresponds to $K(t-\xi) = 1$ when $\alpha = 0,\ \beta = 0$ and with 2T.
2. The dashed line corresponds to $K(t-\xi) = 1 + \frac{(\xi - t)}{\chi}$ when $\alpha = 0,\ \beta = \frac{1}{2}$ and with 2T.
3. The dotted line corresponds to $K(t-\xi) = \xi - t + 1$ when $\alpha = 0,\ \beta = \frac{\chi}{2}$ and with 2T.
4. The dash-dotted line corresponds to $K(t-\xi) = \left[1 + \frac{(\xi - t)}{\chi}\right]^2$ when $\alpha = 1,\ \beta = 1$ and with 2T.
5. The red dash-dot-dot line corresponds to without MDD.
6. The purple dash-dot line corresponds to without 2T.

Figure 2 exhibits the displacement component w of the Stoneley wave w.r.t. ξ for various values of the kernel function of MDD. The variation in the displacement component near the interface of the two mediums changes with the change in the kernel function. The kernel function $K(t-\xi) = 1$ when $\alpha = 0,\ \beta = 0$ shows the higher variation near the interface and starts vanishing as moving away from the interface. However kernel function $K(t-\xi) = \left[1 + \frac{(\xi - t)}{\chi}\right]^2$ when $\alpha = 1,\ \beta = 1$ reduces the variation in the displacement component. So lower the value of the kernel function higher the variation in the displacement component at small values of ξ, as the value of ξ increases, the displacement becomes zero. Moreover, the displacement component shows the opposite behavior without MDD. In addition, as ξ increases, the effect of MDD also decreases.

Figure 3 illustrates the magnitude values of conductive temperature φ w.r.t. ξ for various values of the kernel function of MDD. The variation in the φ near the interface of the two mediums changes with the change of the kernel function. The kernel function $K(t-\xi) = \left[1 + \frac{(\xi - t)}{\chi}\right]^2$ when $\alpha = 1,\ \beta = 1$ shows a higher variation near the interface and starts vanishing as moving away from the interface. So higher the value of the kernel function higher the variation in the conductive temperature at small values of ξ, as the value of ξ increases, the φ becomes zero. Moreover, the φ shows the opposite behavior without MDD. In addition, as ξ increases, the effect of MDD also decreases. However, without two temperature, the φ shows the opposite behavior and decreases sharply near the interface and then become zero. Figure 4 demonstrates the stress component t_{zz} w.r.t. ξ for various values of kernel function of MDD. The variation in the t_{zz} near the interface of the two mediums changes with the change of the kernel function. The kernel function $K(t-\xi) = 1$ when $\alpha = 0,\ \beta = 0$ shows the higher variation near the interface and starts vanishing as moving away from the interface. However kernel function $K(t-\xi) = \left[1 + \frac{(\xi - t)}{\chi}\right]^2$ when $\alpha = 1,\ \beta = 1$ reduces the variation in the t_{zz}. Moreover, the t_{zz} shows the same behavior with high magnitude without MDD. In addition, as ξ increases, the effect of MDD also decreases. So lower the value of the kernel function higher the variation in the t_{zz} at small values of ξ, as the value of ξ increases, the t_{zz} becomes zero.

Figure 5 illustrates the attenuation coefficient w.r.t. ξ for various values of the kernel function of MDD. The variation in the attenuation coefficient near the interface of the two mediums changes with the change

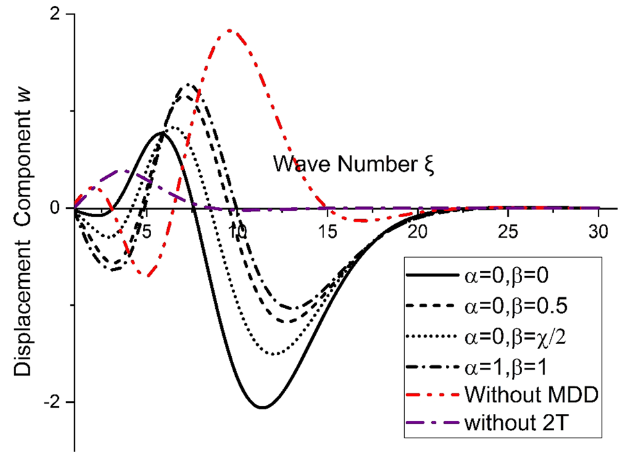

Fig. 2 Deviation of displacement component w of Stoneley waves with MDD

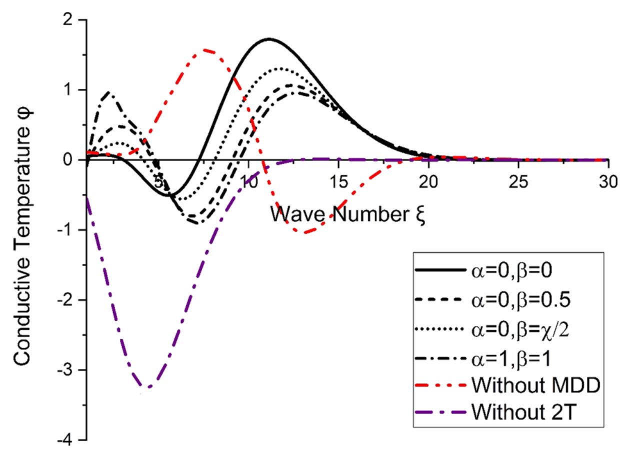

Fig. 3 Deviation of conductive temperature with MDD

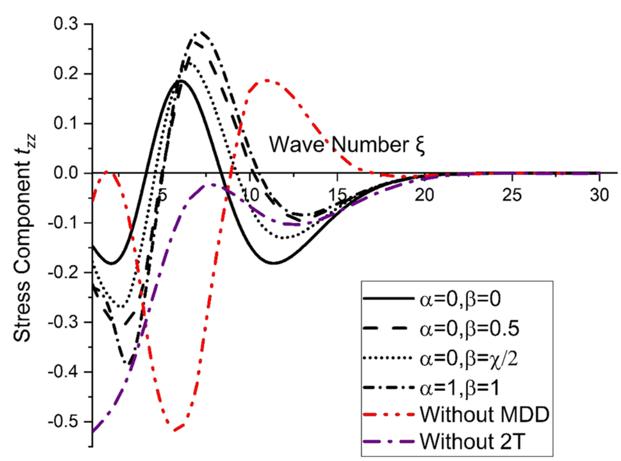

Fig. 4 Deviation of stress component t_{zz} with MDD

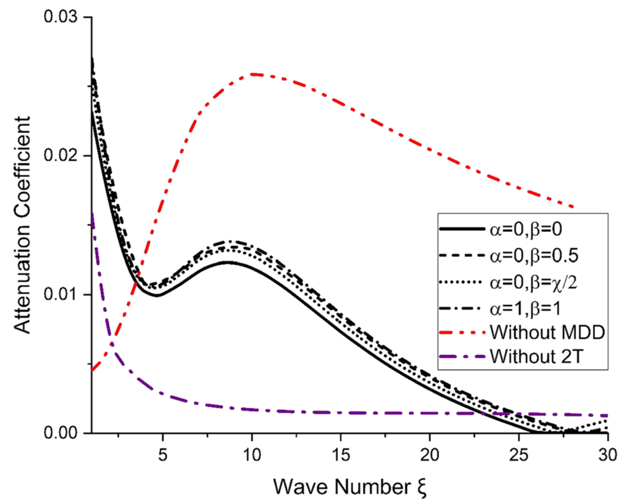

Fig. 5 Deviation of attenuation coefficient of Stoneley waves with MDD

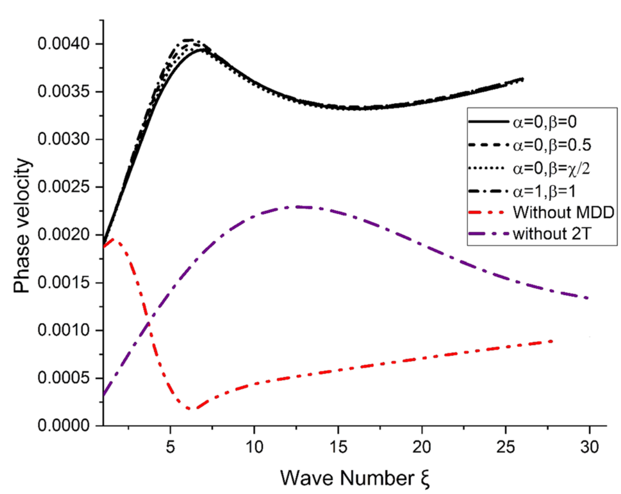

Fig. 6 Deviation of Stoneley waves phase velocity with MDD

in the kernel function. The kernel function $K(t-\xi) = \left[1 + \frac{(\xi-t)}{\chi}\right]^2$ when $\alpha = 1$, $\beta = 1$ shows a higher variation near the interface and starts vanishing as moving away from the interface. So higher the value of the kernel function higher the variation in the attenuation coefficient at small values of ξ, as the value of ξ increases, the attenuation coefficient becomes zero. Moreover, the attenuation coefficient shows the opposite behavior without MDD. In addition, as ξ increases, the effect of MDD also decreases. However, without two temperature, the attenuation coefficient shows the opposite behavior and decreases sharply near the interface and then become zero. Figure 6 illustrates the phase velocity w.r.t. ξ for various values of the kernel function of MDD. The variation in the phase velocity sharply increases near the interface of the two mediums with the change of the kernel function. The kernel function $K(t-\xi) = \left[1 + \frac{(\xi-t)}{\chi}\right]^2$ when $\alpha = 1$, $\beta = 1$ shows a higher variation near the interface and approximately remains the same as moving away from the interface. So higher the value of the kernel function higher the variation in the phase velocity. Moreover, the phase velocity shows the opposite behavior without MDD. However, without two temperature, the phase velocity shows the different behavior and increases sharply near the interface.

8 Conclusion

We bring forth the study of the propagation of the Stoneley wave at the interface of two separate homogeneous transversely isotropic (HTI) thermoelastic mediums with modified GN theory of type II thermoelasticity without energy dissipation, including memory-dependent derivative (MDD) and two temperatures and with rotation. The wave characteristics have been obtained for different Kernel functions of the MDD from the secular equations and are depicted graphically.

Analyzing the graphs revealed the following findings:

- It is also noticed that all the component except the phase velocity of Stoneley waves vanishes away from the interface of the two mediums. In different mediums and at different depths, the characteristics of waves also differ dramatically. MDD and two temperature exhibits a significant influence on the Stoneley wave displacement component, phase velocity, stress component, attenuation coefficient, and temperature distribution at the interface of the two mediums as shown in the figures
- Based on the wave velocity equation, we notice that the change in the kernel function's values causes the dispersion of waves. The resulting Secular equation defines the dispersive property of the Stoneley waves. The problem formulation and numerical results are also approved based on diverse special cases.
- Studying these waves can help us understand geophysics, seismology, ocean physics, SAW devices, and the non-destructive evaluation of structures. Seismological profiles with vertical sections are frequently disturbed by Stoneley waves.

Acknowledgments Not applicable.

Funding No fund/grant/scholarship has been taken for the research work.

Declarations

Conflict of interest The authors declare that they have no conflict of interest.

References

1. Stoneley, R.: Elastic waves at the surface of separation of two solids. Proc. R. Soc. London. Ser. A, Contain. Pap. a Math. Phys. Character. **106**, 416–428 (1924). https://doi.org/10.1098/rspa.1924.0079
2. Scholte, J.G.: The range of existence of Rayleigh and Stoneley waves. Geophys. J. Int. **5**, 120–126 (1947). https://doi.org/10.1111/j.1365-246X.1947.tb00347.x
3. Tajuddin, M.: Existence of Stoneley waves at an unbounded interface between two micropolar elastic half spaces. J. Appl. Mech. **62**, 255–257 (1995)
4. Kumar, R., Devi, S., Abo-Dahab, S.M.: Stoneley waves at the boundary surface of modified couple stress generalized thermoelastic with mass diffusion. J. Appl. Sci. Eng. **21**, 1–8 (2018). https://doi.org/10.6180/jase.201803_21(1).0001
5. Ting, T.C.T.: Surface waves in a rotating anisotropic elastic half-space. Wave Motion **40**, 329–346 (2004). https://doi.org/10.1016/j.wavemoti.2003.10.005
6. Abo-Dahab, S.M.: Surface waves in coupled and generalized thermoelasticity. In: Encyclopedia of Thermal Stresses. pp. 4764–4774. Springer Netherlands, Dordrecht (2014)
7. Abo-Dahab, S.: Propagation of Stoneley waves in magneto-thermoelastic materials with voids and two relaxation times. J. Vib. Control. **21**, 1144–1153 (2015). https://doi.org/10.1177/1077546313493651
8. Kumar, R., Sharma, N., Lata, P., Marin, M.: Reflection of plane waves at micropolar piezothermoelastic half-space. Comput. Methods Sci. Technol. **24**, 113–124 (2018). https://doi.org/10.12921/cmst.2016.0000069
9. Abd-Alla, A.M., Abo-Dahab, S.M., Khan, A.: Rotational effect on thermoelastic Stoneley, Love and Rayleigh waves in fibre-reinforced anisotropic general viscoelastic media of higher order. Struct. Eng. Mech. **61**, 221–230 (2017). https://doi.org/10.12989/sem.2017.61.2.221
10. Singh, S., Tochhawng, L.: Stoneley and Rayleigh waves in thermoelastic materials with voids. J. Vib. Control. **25**, 2053–2062 (2019). https://doi.org/10.1177/1077546319847850
11. Kaur, I., Lata, P.: Stoneley wave propagation in transversely isotropic thermoelastic medium with two temperature and rotation. GEM Int. J. Geomath. **11**, 1–17 (2020). https://doi.org/10.1007/s13137-020-0140-8
12. Lata, P., Himanshi: Stoneley wave propagation in an orthotropic thermoelastic media with fractional order theory. Compos. Mater. Eng. **3**, 57 (2021)
13. Kaur, I., Lata, P., Singh, K.: Reflection of plane harmonic wave in rotating media with fractional order heat transfer and two temperature. Partial Differ. Equ. Appl. Math. **4**, 100049 (2021). https://doi.org/10.1016/J.PADIFF.2021.100049
14. Lata, P., Kaur, I., Singh, K.: Reflection of plane harmonic wave in transversely isotropic magneto-thermoelastic with two temperature, rotation and multi-dual-phase lag heat transfer. (2021)

15. Kaur, I., Singh, K.: Plane wave in non-local semiconducting rotating media with Hall effect and three-phase lag fractional order heat transfer. Int. J. Mech. Mater. Eng. **16**, 1–16 (2021). https://doi.org/10.1186/S40712-021-00137-3/FIGURES/16
16. Lata, P., Kaur, I., Singh, K.: Propagation of plane wave in transversely isotropic magneto-thermoelastic material with multi-dual-phase lag and two temperature. Coupled Syst. Mech. **9**, 411–432 (2020). https://doi.org/10.12989/csm.2020.9.5.411
17. Wang, J.-L., Li, H.-F.: Surpassing the fractional derivative: Concept of the memory-dependent derivative. Comput. Math. Appl. **62**, 1562–1567 (2011). https://doi.org/10.1016/j.camwa.2011.04.028
18. Yu, Y.-J., Hu, W., Tian, X.-G.: A novel generalized thermoelasticity model based on memory-dependent derivative. Int. J. Eng. Sci. **81**, 123–134 (2014). https://doi.org/10.1016/j.ijengsci.2014.04.014
19. Ezzat, M.A., El-Karamany, A.S., El-Bary, A.A.: Generalized thermo-viscoelasticity with memory-dependent derivatives. Int. J. Mech. Sci. **89**, 470–475 (2014). https://doi.org/10.1016/j.ijmecsci.2014.10.006
20. Ezzat, M.A., El-Karamany, A.S., El-Bary, A.A.: A novel magneto-thermoelasticity theory with memory-dependent derivative. J. Electromagn. Waves Appl. **29**, 1018–1031 (2015). https://doi.org/10.1080/09205071.2015.1027795
21. Ezzat, M.A., El-Karamany, A.S., El-Bary, A.A.: Generalized thermoelasticity with memory-dependent derivatives involving two temperatures. Mech. Adv. Mater. Struct. **23**, 545–553 (2016). https://doi.org/10.1080/15376494.2015.1007189
22. Ezzat, M.A., El Karamany, A.S., El-Bary, A.A.: Thermoelectric viscoelastic materials with memory-dependent derivative. Smart Struct. Syst. **19**, 539–551 (2017). https://doi.org/10.12989/sss.2017.19.5.539
23. Kaur, I., Lata, P., Singh, K.: Memory-dependent derivative approach on magneto-thermoelastic transversely isotropic medium with two temperatures. Int. J. Mech. Mater. Eng. (2020). https://doi.org/10.1186/s40712-020-00122-2
24. Kaur, I., Lata, P., Singh, K.: Reflection and refraction of plane wave in piezo-thermoelastic diffusive half spaces with three phase lag memory dependent derivative and two-temperature. Waves Random Complex Media (2020). https://doi.org/10.1080/17455030.2020.1856451
25. Kaur, I., Lata, P., Singh, K.: Effect of memory dependent derivative on forced transverse vibrations in transversely isotropic thermoelastic cantilever nano-Beam with two temperature. Appl. Math. Model. **88**, 83–105 (2020). https://doi.org/10.1016/j.apm.2020.06.045
26. Kaur, I., Lata, P., Handa, K.: Effects of Memory Dependent Derivative of Bio-heat Model in Skin Tissue exposed to Laser Radiation. EAI Endorsed Trans. Pervasive Heal. Technol. **6**, 164589 (2020). https://doi.org/10.4108/eai.13-7-2018.164589
27. Marin, M.: On weak solutions in elasticity of dipolar bodies with voids. J. Comput. Appl. Math. **82**, 291–297 (1997). https://doi.org/10.1016/S0377-0427(97)00047-2
28. Golewski, G.L.: Fracture performance of cementitious composites based on quaternary blended cements. Materials (Basel). **15**, 6023 (2022). https://doi.org/10.3390/ma15176023
29. Marin, M., Öchsner, A., Craciun, E.M.: A generalization of the Saint-Venant's principle for an elastic body with dipolar structure. Contin. Mech. Thermodyn. **32**, 269–278 (2020). https://doi.org/10.1007/s00161-019-00827-6
30. Marin, M., Öchsner, A., Craciun, E.M.: A generalization of the Gurtin's variational principle in thermoelasticity without energy dissipation of dipolar bodies. Contin. Mech. Thermodyn. **32**, 1685–1694 (2020). https://doi.org/10.1007/s00161-020-00873-5
31. Kaur, I., Singh, K., Ghita, G.M.D.: New analytical method for dynamic response of thermoelastic damping in simply supported generalized piezothermoelastic nanobeam. ZAMM - J. Appl. Math. Mech. / Zeitschrift für Angew. Math. und Mech. **101**, (2021). https://doi.org/10.1002/zamm.202100108
32. Golewski, G.L.: Strength and microstructure of composites with cement matrixes modified by fly ash and active seeds of C-S-H phase. Struct. Eng. Mech. **82** (2022). https://doi.org/10.12989/sem.2022.82.4.543
33. Golewski, G.L.: On the special construction and materials conditions reducing the negative impact of vibrations on concrete structures. Mater. Today Proc. **45**, 4344–4348 (2021). https://doi.org/10.1016/j.matpr.2021.01.031
34. Trivedi, N., Das, S., Craciun, E.-M.: The mathematical study of an edge crack in two different specified models under time-harmonic wave disturbance. Mech. Compos. Mater. **58**, 1–14 (2022). https://doi.org/10.1007/s11029-022-10007-4
35. Zhang, P., Han, S., Golewski, G.L., Wang, X.: Nanoparticle-reinforced building materials with applications in civil engineering. Adv. Mech. Eng. **12**, 168781402096543 (2020). https://doi.org/10.1177/1687814020965438
36. Sur, A., Kanoria, M.: Modeling of memory-dependent derivative in a fibre-reinforced plate. Thin-Walled Struct. (2018). https://doi.org/10.1016/j.tws.2017.05.005
37. Golewski, G.L.: An extensive investigations on fracture parameters of concretes based on quaternary binders (QBC) by means of the DIC technique. Constr. Build. Mater. **351**, 128823 (2022). https://doi.org/10.1016/j.conbuildmat.2022.128823
38. Golewski, G.L.: Comparative measurements of fracture toughgness combined with visual analysis of cracks propagation using the DIC technique of concretes based on cement matrix with a highly diversified composition. Theor. Appl. Fract. Mech. **121**, 103553 (2022). https://doi.org/10.1016/j.tafmec.2022.103553
39. Gupta, S., Das, S., Dutta, R., Verma, A.K.: Higher-order fractional and memory response in nonlocal double poro-magneto-thermoelastic medium with temperature-dependent properties excited by laser pulse. J. Ocean Eng. Sci. (2022). https://doi.org/10.1016/j.joes.2022.04.013
40. Chandrasekharaiah, D.S.: Hyperbolic thermoelasticity: a review of recent literature. Appl. Mech. Rev. **51**, 705–729 (1998). https://doi.org/10.1115/1.3098984
41. Green, A.E., Naghdi, P.M.: On undamped heat waves in an elastic solid. J. Therm. Stress. **15**, 253–264 (1992). https://doi.org/10.1080/01495739208946136
42. Schoenberg, M., Censor, D.: Elastic waves in rotating media. Q. Appl. Math. **31**, 115–125 (1973). https://doi.org/10.1090/qam/99708
43. Youssef, H.M.: Theory of two-temperature thermoelasticity without energy dissipation. J. Therm. Stress. **34**, 138–146 (2011). https://doi.org/10.1080/01495739.2010.511941
44. Bachher, M.: Plane harmonic waves in thermoelastic materials with a memory-dependent derivative. J. Appl. Mech. Tech. Phys. **60**, 123–131 (2019). https://doi.org/10.1134/S0021894419010152

45. Slaughter, W.S.: The Linearized Theory of Elasticity. Birkhäuser Boston, Boston (2002)
46. Kumar, R., Sharma, N., Lata, P., Abo-Dahab, S.M.: Mathematical modelling of Stoneley wave in a transversely isotropic thermoelastic media. **177005**, 78–103 (2010)

Publisher's Note Springer Nature remains neutral with regard to jurisdictional claims in published maps and institutional affiliations.